Modelling of Inverter Heat Pumps in TRNSYS

Fabian Hüsing[1] and Peter Pärisch[1]

[1] Institute for Solar Energy Research Hamelin (ISFH)

Abstract

Validated simulation models are important for the development of advanced system design and control strategies. In this contribution we present an approach to model inverter heat pumps by combination of multiple single speed models in TRNSYS. Performance data of a brine/water heat pump is determined by experimental investigations for three levels of inverter frequency. Deviation in efficiency is observed at source temperatures above 10 °C, with lower inverter frequencies reaching higher coefficients of performance. Each level of inverter frequency is modelled with one instance of TRNSYS Type 401. To validate the modelling approach, we use experimental data of load variations. Relative deviations show an overestimation of heat transferred at condenser of $\Delta Q_{cond,rel} = 3.7\ \%$ and electric energy used at compressor of $\Delta P_{el,rel} = 2\ \%$ in the simulation Overall, the approach is able to represent the operational behavior of an inverter heat pump and can be suggested for system control strategy development by means of simulations.

Keywords: inverter heat pump, performance data, TRNSYS model, experimental validation

1. Introduction

Scenarios for an efficient and feasible transformation towards a fully renewable energy supply system identify electric compression heat pumps (hereafter HP) as a key technology (Bründlinger et al. 2018, Gebert et al. 2018, Henning & Palzer 2013). This assessment is based on several characteristic features. HP contribute to an integrated energy supply by linking the electricity and heat sectors. Efficient heat generation as well as opportunities for connection of thermal storage capacity and demand management are important in this context. Furthermore, HP operate at a decentralized level, as they gain a high percentage of the heat they provide in their vicinity. Therefore, use of HP contributes to an even allocation of energy processing units.

Inverter heat pumps are able to modify their heat output and demand for electric power by changing the rotational speed of the compressor and aperture of expansion valves. Therefore, they add an important degree of freedom regarding optimized control of heat pump systems. Especially systems with generation of electricity on site and/or complex heat source designs are expected to benefit from optimized control strategies.

In development and optimization of system design and control strategies numeric simulations are an established tool. To evaluate the potentials of inverter heat pumps in differently configured heating systems, it is crucial to use component models validated with experimental data.

2. Experiment and Simulation

In this contribution we present experimental investigations performed on a commercially available heat pump and propose an approach to model inverter heat pumps in TRNSYS (Klein et al. 2010). For detailed analysis a dynamic load cycle is measured and used for validation of the proposed modelling approach.

Identification of heat pump parameters

Performance data for the HP is determined under steady state operation conditions. A brine/water HP (hereafter BWHP) is tested for the parameter set described in Table 1 based on the procedure defined in parts 2 and 3 of DIN EN 14511 standard. The aim is to identify performance data for a wide range of evaporator inlet and condenser outlet temperatures ($T_{evap,in}$ and $T_{cond,out}$) at different partial loads (inverter frequencies).

doi:10.18086/eurosun.2020.04.08 Available at http://proceedings.ises.org

Table 1: Brine/Water HP - parameter set tested

$T_{evap,in}$	$T_{cond,out}$	f
°C	°C	Hz
-5	35	30
0		
5	45	60
10		
15	55	90
20		

Figure 1 depicts a schematic of the experimental setup used for the investigation. A fluid circuit with a resistance heater is connected to the evaporator of the BHWP to operate as a heat source. The source circuit is filled with brine. The condenser of the BHWP is connected to a fluid circuit filled with water, operating as a heat sink. The sink circuit is coupled to a chilled water distributing network over a heat exchanger and includes a resistance heater. The setup allows heat supply at the source circuit and heat extraction and supply at the sink circuit and therefore, control of inlet temperatures at evaporator and condenser. Heat source and sink temperatures at the inlet and outlet of the evaporator and condenser are measured with calibrated Pt100 immersion temperature sensor couples (uncertainty of measurement: ±0.10 K for temperature, ±0.04 K for temperature difference). Mass flows through the evaporator and condenser are measured with Coriolis mass flow meters (uncertainty of measurement: ±0.17 %). Electrical power at the BWHP compressor is measured with a power analyzer (uncertainty of measurement: ±0.47 %).

Steady state operation conditions (deviations of state variables smaller than defined in Table 4 of DIN EN 14511:2013 Part 3) are captured over thirty minutes at a measurement interval of six seconds for each combination of parameters in Table 1. For each combination of inverter frequency and condenser outlet temperature, mass flows in evaporator and condenser circuits ($\dot{m}_{cond}$ und $\dot{m}_{evap}$) are determined at nominal conditions given in Tables 7, 8 and 9 of DIN EN 14511:2013 Part 2, which define evaporator and condenser in- and outlet temperatures. All other evaporator inlet temperature levels are tested at same mass flows for given combinations of inverter frequency and condenser outlet temperature, resulting in different evaporator outlet and condenser inlet temperatures.

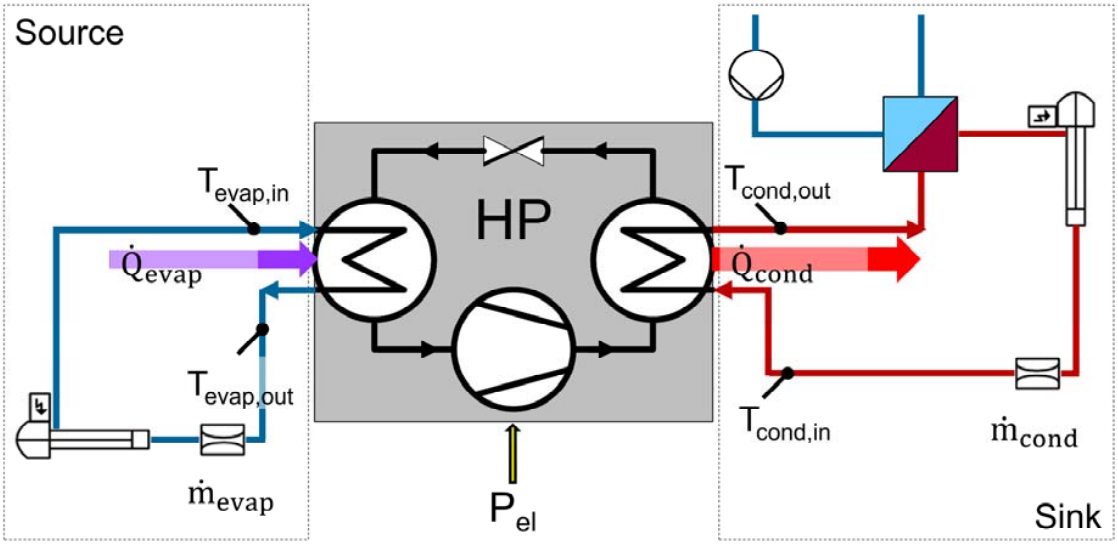

Figure 1: Schematic testing environment for experimental investigation

The heat flux transferred at the condenser is calculated according to Equation (1).

$$\dot{Q}_{cond} = \dot{m}_{cond} * c_p * (T_{cond,out} - T_{cond,in}) \qquad \text{(Equation. 1)}$$

$\dot{Q}_{cond}$ = heat flux transferred to sink circuit at condenser; $\dot{m}_{cond}$ = mass flow at condenser; c_p = specific heat capacity; $T_{cond,in}$ = condenser inlet temperature; $T_{cond,out}$ = condenser outlet temperature

In Figure 2 the condenser heat flux is plotted against the evaporator inlet temperature for different condenser outlet temperatures and inverter frequencies. The inverter frequency is distinguished by color (green ≙ 30 Hz, blue ≙ 60 Hz and orange ≙ 90Hz). Darker shades correspond to higher temperatures at the condenser outlet. At 30 Hz inverter frequency and a condenser outlet temperature of 55 °C, steady state conditions are not reached.

The condenser heat flux increases with inverter frequency and source temperature. For most of the data, higher heating powers are reached at lower condenser outlet temperatures. Heating powers between 1.6 kW and 9.5 kW are recorded. At an inverter frequency of 90 Hz the heating power shows weaker increase at evaporator inlet temperatures above 10 °C for condenser outlet temperatures of 35 °C and 45 °C.

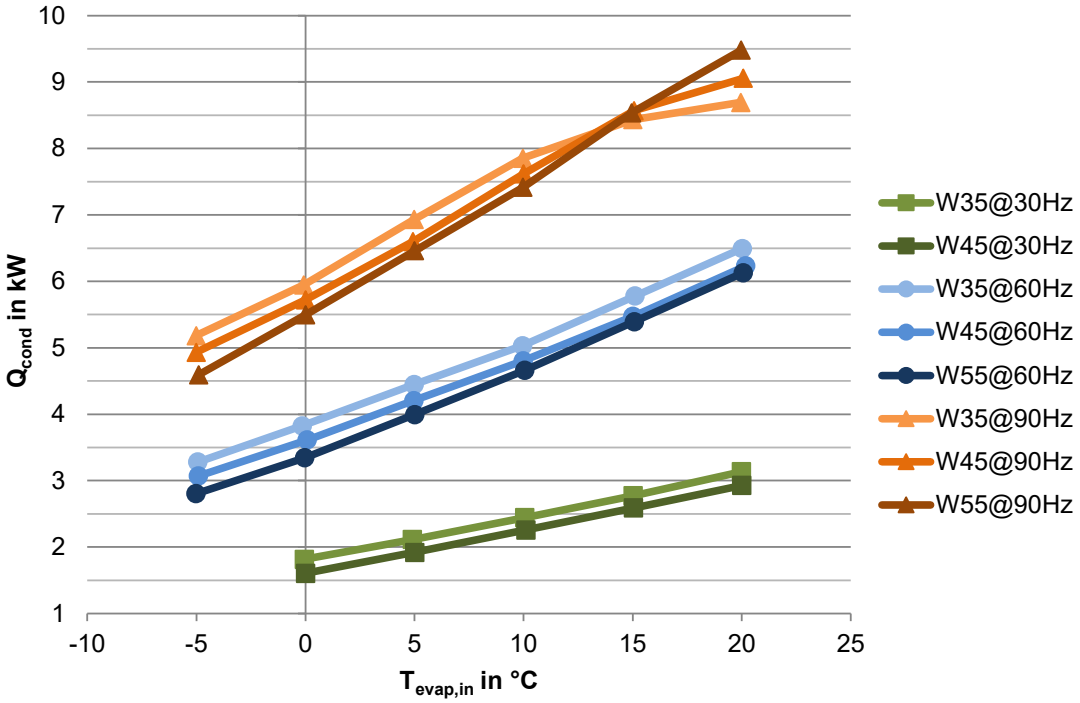

Figure 2: Condenser heat flux over source temperature

The coefficient of performance (COP) is calculated according to Equation (2). In contrast to DIN EN 14511:2013, no electric power for pumps or controller are considered. This is due to the fact, that these components are individually considered in TRNSYS simulations and are thus not needed for parameterization of the model.

$$COP = \frac{\sum_\tau \dot{Q}_{cond}}{\sum_\tau P_{el}} \qquad \text{(Equation 2)}$$

COP = coefficient of performance; P_{el} = electrical power of the BWHP compressor; τ = time period of stationary measurement

Figure 3 depicts the COP as function of the evaporator inlet temperature for different condenser outlet temperatures and inverter frequencies. The coloring is analog to Figure 2. Determined COP reach values from 2.47 to 8.86. In general, higher COP are achieved at higher evaporator inlet temperatures. In the following the influence of the inverter frequency is discussed at a condenser outlet temperature of 35 °C (upper three graphs). At low evaporator inlet temperatures small differences in COP are observed. With increasing evaporator inlet temperature, larger differences occur. At evaporator inlet temperatures above 10 °C, the increase of COP at 90 Hz shows a decreasing trend, while at 60 Hz linear and at 30 Hz exponential increase is observed. This leads to a large divergence in COP at the highest source temperature ($COP_{B20W35@30Hz}$ = 8.86 versus $COP_{B20W35@90Hz}$ = 5.33).

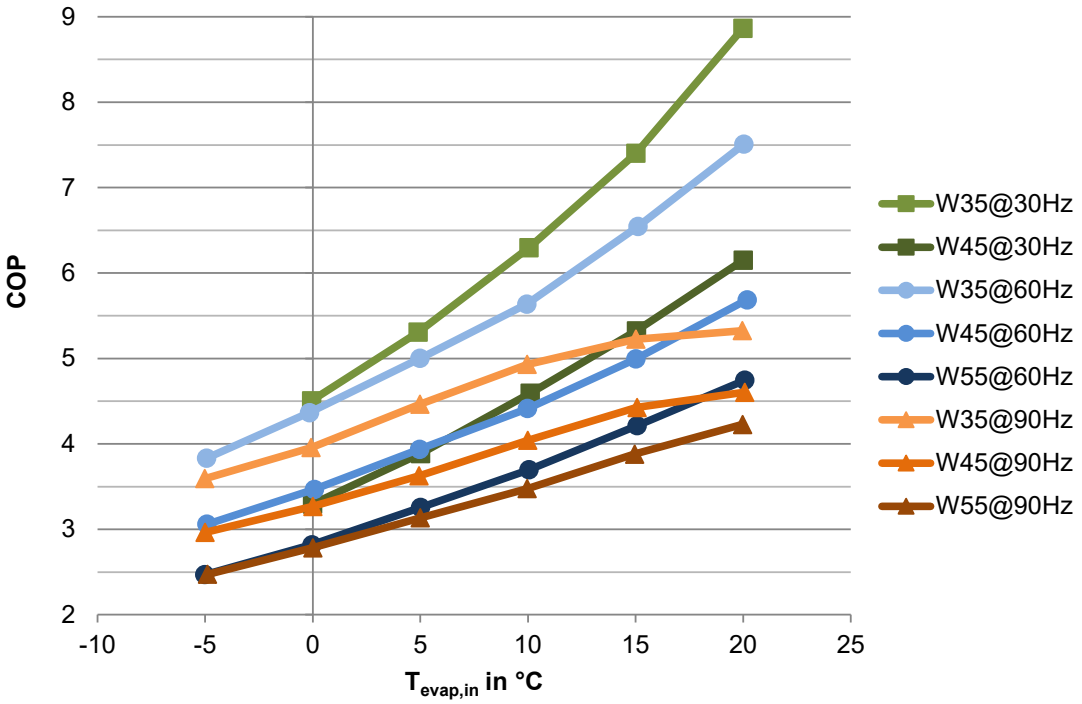

Figure 3: Coefficient of performance (COP) over source temperature Modelling approach

To reproduce the performance of a HP at various inverter frequencies a TRNSYS model is developed. TRNSYS Type 401 (Afjei & Winter, 1997), which calculates the condenser heat flux and electric power based on the evaporator inlet and condenser outlet temperatures by a biquadratic polynomial, is used. We choose the approach to combine multiple instances of Type 401, first presented in (Hüsing et al. 2018). Each instance of Type 401 is parameterized with polynomial coefficients derived from the performance data at one inverter frequency, thus modelling one load level. Outputs for all load levels are simultaneously calculated throughout the simulations. To obtain the conditions for a given inverter frequency, linear interpolation between results of adjacent load levels is implemented.

For the BWHP three instances of Type 401 are used to calculate results for operation at 30, 60 and 90 Hz inverter frequency. In Figure 4 the structure of the model in TRNSYS simulation studio is shown. Input variables, either from data files or a surrounding system simulation, supplied to all three instances are evaporator and condenser inlet temperatures as well as mass flows. Each instance calculates its output variables. The most important output variables are evaporator and condenser powers and outlet temperatures, as well as compressor power. The output variables are connected to the Equation block “HP_Output”, where the interpolation, based on the inverter frequency is performed. The inverter frequency is supplied to the “HP_Output” equation block and may be derived from measurement data or obtained using different control strategies.

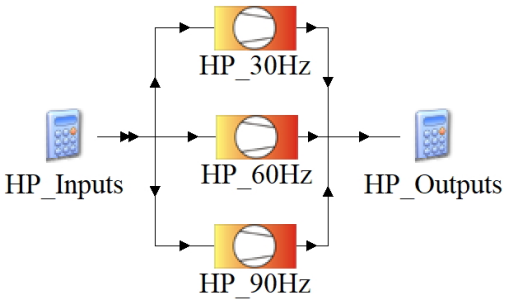

Figure 4: Structure of inverter heat pump model in TRNSYS Simulation Studio

The heat capacity of the heat pump condenser is important for accurate modelling of dynamic operation (Mercker et al. 2014). In Type 401 it is regarded via time constants for heating up and cooling down (Afjei & Winter, 1997). For the presented model we assume, that the time constant for cooling down ($\tau_{cooling} = 45$ s) is not influenced by inverter frequency. We assume the time constant for heating up to be inversely proportional to inverter frequency, as the heat flow is nearly proportional to the inverter frequency and the total heat capacity does not change. The time

constants are calculated according to Equation (3), with $\tau_{heating}(f_{ref}) = 30$ s at $f_{ref} = 90\ Hz$.

$$\tau_{heating}(f) = \frac{f_{ref}}{f} * \tau_{heating}(f_{ref}) \qquad \text{(Equation 3)}$$

$\tau_{heating}(f)$ = inverter frequency dependent time constant for heating thermal inertia of the condenser; f = inverter frequency; $\tau_{heating}(f_{ref})$ = time constant for heating at reference inverter frequency

Temperatures and heating rates for all partial loads and the interpolated results can be monitored by online plotters throughout the simulation. The proposed approach allows the replacement of single component HP models in existing system simulation models by connections to the "HP_Input" and "HP_Output" blocks.

Validation against experimental data

To validate the modelling approach, we use data from experiments with load variations. The experiment is carried out in the setup described above and shown in Figure 1. At set points for the evaporator inlet ($T_{evap,in}$ = 10 °C) and condenser outlet temperature ($T_{cond,out}$ = 45 °C), the inverter frequency is varied in steps of 60; 75; 90; 80 Hz. Corresponding to each variation in inverter frequency, the condenser outlet temperature changes. After reaching steady state, the condenser inlet temperature is adjusted to reach a condenser outlet temperature $T_{cond,out}$ = 45 °C. Thus, intervals of with small variation of condenser temperatures (± 2 K) are recorded. In Figure 5 temporal progress of inverter frequency during the experiment is depicted.

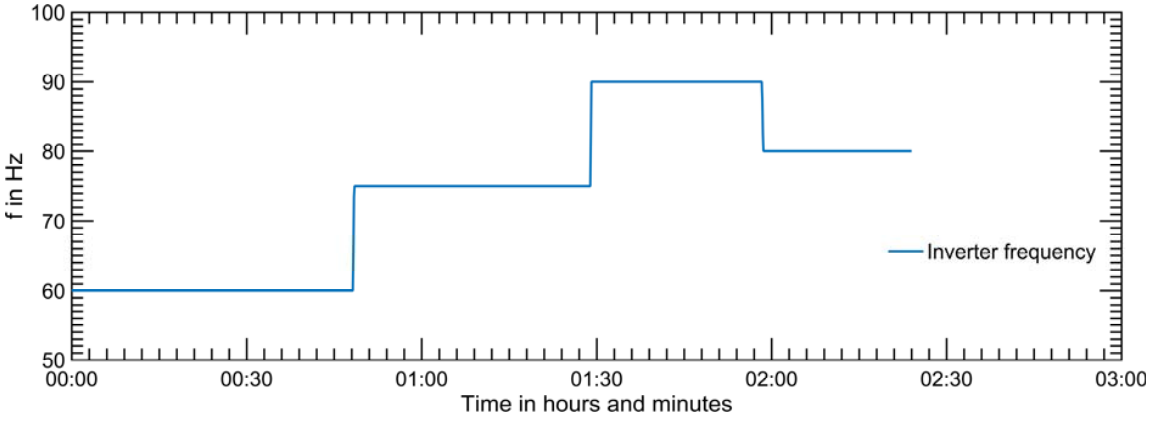

Figure 5: Temporal progression of inverter frequency

We use the modelling approach described in the previous paragraph to simulate the load variations. Therefore, measured data for evaporator and condenser inlet temperatures and mass flows, as well as the inverter frequency are supplied to the model. Throughout the simulation temporal progresses of evaporator and condenser outlet temperatures and heat fluxes as well as electric power at the compressor are recorded in a data file. Subsequently the simulation outputs are compared to the measured data, to assess the accuracy of the modelling approach.

In Figure 6 temperatures are plotted against time. Due to the larger deviations in outlet temperatures at the beginning of the simulation, induced by initial conditions, the first two minutes are not considered for the subsequent analysis. The upper plot shows the evaporator inlet temperature and the measured as well as simulated evaporator outlet temperature. The temporal progress shows good agreement for the simulated evaporator outlet temperature. Maximum deviation of -0.89 K is observed, while a mean deviation of -0.06 K is achieved. The lower plot shows the condenser inlet temperature and the measured as well as the simulated condenser outlet temperatures. Mean deviation of 0.07 K and maximum deviation of 1.78 K are slightly larger than those at the evaporator. Still a good agreement in temporal progress can be confirmed.

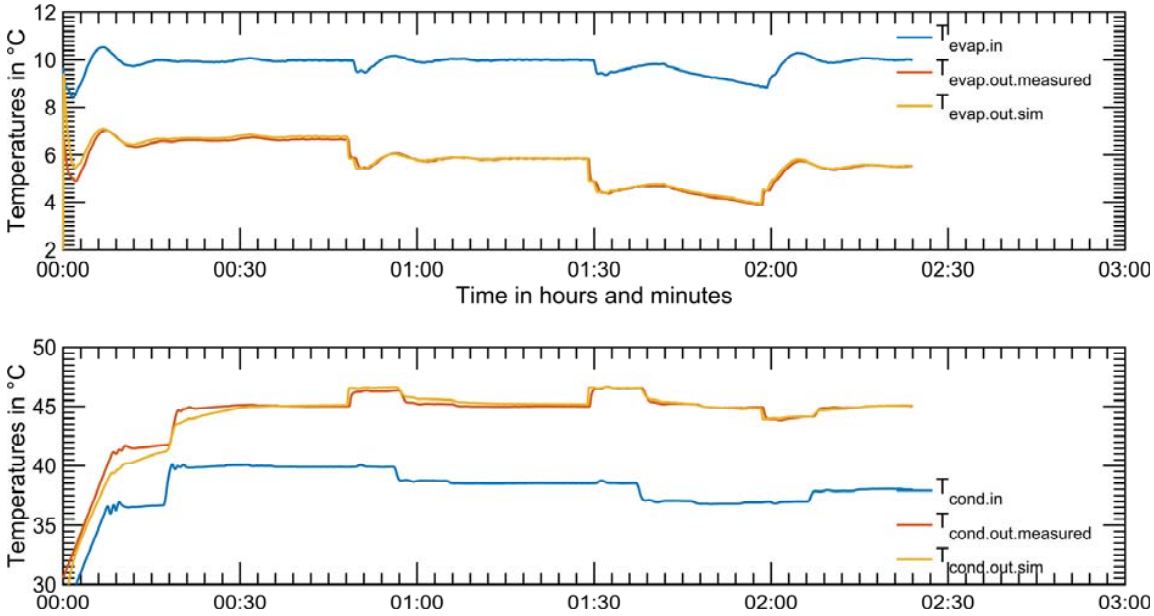

Figure 6: Measured and simulated evaporator and condenser temperatures over time

In Figure 7 the flows of heat at condenser (top) and electric power (bottom) are plotted against the time. While the levels of condenser heat flux are well represented in the simulation, single fluctuations which occurred during the measurement are not reproduced by the simulation model. These fluctuations can be attributed to unevenly distribution of temperatures and thermal inertia of the heat carrier in the sink circuit. As the distribution of heat capacity of the heat carrier is not modelled (only one temperature node for the circuit in Type 401) further extensions are needed for a more accurate representation. In the time interval shortly after changes in inverter frequency, we observe that the temperatures and heat flux changes are more directly in the simulation than in the measurement. This is attributed to a change in condenser outlet temperature, which in reality is delayed by the thermal inertia of the condenser. Because in simulation all load levels are computed in parallel, the change in inverter frequency shows immediate effect on the interpolated output variables.

The temporal progress of electric power shows good agreement between measurement and simulation. Integral quantities for heat transferred at condenser and electric energy used at compressor are calculated according to Equations (4) and (5) for measured and simulated data.

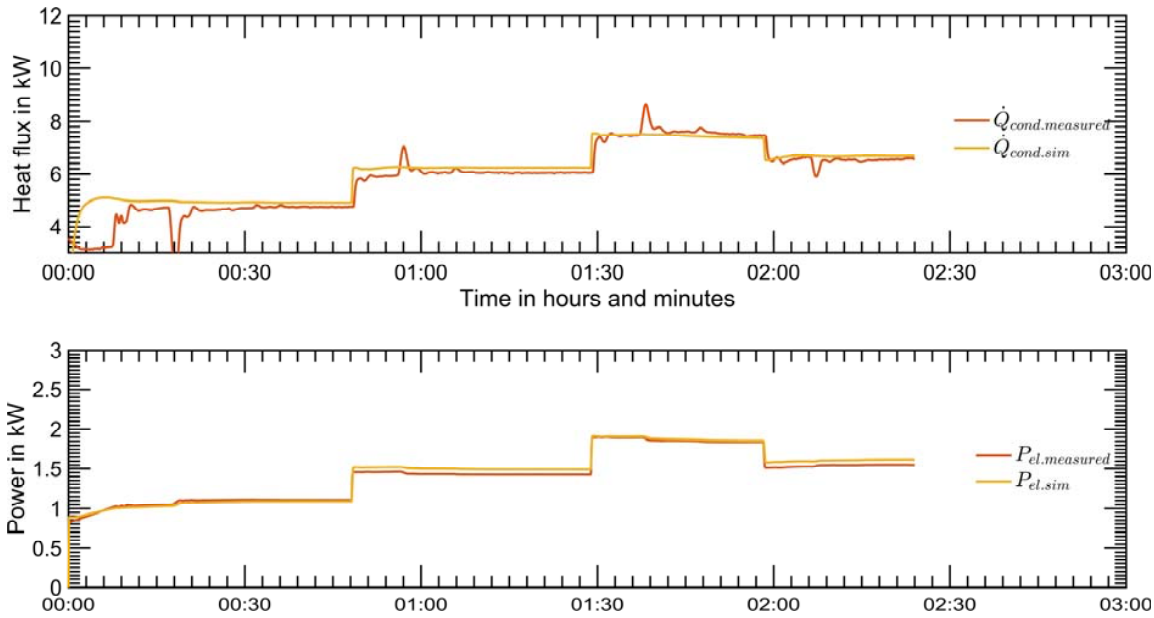

Figure 7: Measured and simulated heat fluxes and powers over time

$$Q_{cond} = \sum_{\tau} \dot{Q}_{cond} * \Delta\tau \quad \text{(Equation 4)}$$

Q_{cond} = heat energy transferred to the sink circuit at condenser; $\dot{Q}_{cond}$ = heat flux transferred to the sink circuit at condenser; τ = time period of the measurement; $\Delta\tau$ = time interval of the measurement

$$W_{el} = \sum_{\tau} P_{el} * \Delta\tau \quad \text{(Equation 5)}$$

W_{el} = electric energy used at compressor; P_{el} = electric power used at compressor; τ = time period of measurement; $\Delta\tau$ = time interval of the measurement

Amounts of heat transferred at condenser are $Q_{cond,measured} = 14.11\ kWh$ and $Q_{cond,SIM} = 14.64\ kWh$, respectively. For the electric energy used at the compressor $P_{el,measured} = 3.40\ kWh$ and $P_{el,SIM} = 3.47\ kWh$ result. Relative deviations are calculated according to Equation (6) and show an overestimation of heat $\Delta Q_{cond,rel} = 3.7\ \%$ and $\Delta P_{el,rel} = 2\ \%$ in the simulation. Hence, the performance of the BWHP is overestimated by $\Delta COP = 3.1\ \%$.

$$\Delta E_{rel} = \frac{(E_{sim} - E_{measured})}{E_{measured}} \quad \text{(Equation 6)}$$

ΔE_{rel} = relative deviation in energy between measurement and simulation; E_{sim} = simulated energy quantity (Q_{cond} or W_{el}); $E_{measured}$ = measured energy quantity

3. Discussion

Performance data of a BWHP is successfully determined by experimental investigation. The data shows large influence of inverter frequency on efficiency. Especially at higher source temperatures (above 10 °C) the operation at lower inverter frequencies induces significantly higher coefficients of performance. Therefore, selection of inverter frequency is a crucial factor for the control of heat pump systems. We expect especially solar assisted HP systems (solar heat sources - high source temperatures and/or solar electricity – demand management) with inverter heat pumps to benefit from sophisticated control strategies.

A trend to decreasing heating power at high source temperatures and maximum inverter frequency is observed. This may be attributed to one of the inner components of the HP (compressor, expansion valve, heat exchangers) reaching a physical limit. More detailed analysis of the inner cycle could provide better insight.

An approach to model inverter heat pumps by use of multiple instances of TRNSYS Type 401 is presented. In best-case this would allow to model inverter HP by performance data available from certified testing (e.g. DIN EN 14825:2018).

The validation concerning frequency variation and small temperature variations at the operating point B10W45 shows good agreement in temporal progress of the decisive variables (outlet temperatures and energy fluxes). Relative deviations of energy quantities are below 4 %. The deviation corresponds well with modelling of single speed heat pump without mass flow correction (Pärisch et al. 2014).

Larger deviations are observed shortly after changes of inverter frequency or inlet temperature. This emphasizes the importance of the thermal inertia of the condenser (heat up time constant), which is not yet a part of performance data provided by certified testing. The presented approach is not able to model effects of thermal inertia in cases of temperature changes resulting from inverter frequency modification.

Overall the approach is able to represent the operational behavior of inverter heat pumps. Therefore, it can be used for system control strategy development by means of simulations.

4. Outlook

Our current work aims at validating the modeling approach with a broader range of boundary conditions, such as lower inverter frequencies and temperature variation over larger ranges.

In ongoing research, the presented approach is applied to model an air/water HP. Experimental investigations are carried out at a new modular heat pump test facility at ISFH. The new facility is designed to enable heat pump testing at wider ranges of temperatures and mass flows than the setup used for the investigations in this contribution.

5. Acknowledgments

The presented works result from research projects funded by the state of Lower Saxony and the European Union (contract no. ZW 6-85037507) as well as the German Federal Ministry of Economy and Energy (contract no. 03ET1275A). The authors are grateful for the support of their work. The content of this publication is the sole responsibility of the authors.

Special appreciation is also expressed to Ms. Marie Kreye, who largely contributed to the presented results in the frame of her bachelor thesis.

6. References

Afjei, T. and Wetter, M. 1997. Compressor Heat Pump Including Frost and Cacle Losses, Version 1.1 Model Description and Implenmenting into TRNSYS, Zentralschweizerisches Technikum Luzern, Horw

Bründlinger T., König J. E., Frank O., Gründig D., Jugel C., Kraft P., Krieger O., Mischinger S., Prein P., Seidl H., Siegemund S., Stolte C., Teichmann M., Willke J., Wolke M. 2018. dena-Leitstudie Integrierte Energiewende – Ergebnisbericht und Handlungsempfehlungen, Herausgeber: Deutsche Energie-Agentur GmbH (dena), Berlin

DIN EN 14511:2013-12, Air conditioners, liquid chilling packages and heat pumps for space heating and cooling and process chillers, with electrically driven compressors – Parts 2 and 3, German version EN 14511:2013, Beuth Verlag, Berlin, 2013

DIN EN 14825:2019-07, Air conditioners, liquid chilling packages and heat pumps, with electrically driven compressors, for space heating and cooling - Testing and rating at part load conditions and calculation of seasonal performance; German version EN 14825:2018, Beuth Verlag, Berlin, 2019

Gebert P., Herhold P., Burchard J., Schönberger S., Rechenmacher F. Kirchner A., Kemmler A. and Wünsch M. 2018. Klimapfade für Deutschland – Study by Boston Consulting Group and Prognos on behalf of the Bundesverband der Deutschen Industrie (BDI) e.V., Berlin

Henning H.-M. and Palzer A. 2013. Energiesystem Deutschland 2050, Fraunhofer-Institut für Solare Energiesysteme ISE, Freiburg

Hüsing F., Mercker O., Hirsch H., Kuntz D., Walker-Hertkorn S., Sabel M. 2018. Horizontal ground heat exchangers and solar collectors as optimized bivalent heat source for highly efficient heat pump systems, Final report (german language), Institut für Solarenergieforschung, Hameln, https://doi.org/10.2314/GBV:1047633868

Mercker, O., Pärisch, P. and Rockendorf G. 2014. Taktverhalten von Sole/Wasser-Wärmepumpen – Messung der thermischen Zeitkonstanten und ihre Bedeutung für die Jahresarbeitszahl, Proceedings of BauSIM 2014 - Fifth German-Austrian IBPSA Conference, RWTH Aachen University, Aachen

Pärisch P., Mercker O., Warmuth J., Tepe R., Bertram E., Rockendorf G. 2014. Investigation and model validation of a ground-coupled heat pump for the combination with solar collectors; in Applied Thermal Energy Volume 62, Issue 2 (2014) P. 375-381, Elsevier, München

Klein S.A., et al., 2010. TRNSYS 17. A Transient System Simulation Program, Solar Energy Laboratory, University of Wisconsin, Madison, USA, http://sel.me.wisc.edu/trnsys